Iontophoretic fraction collection for Coupling Capillary Zone Electrophoresis with Matrix-assisted Laser Desorption/Ionization Mass Spectrometry

*Jean-Marc Busnel, Jacques Josserand, Niels Lion, Hubert H. Girault**

Laboratoire d'Electrochimie Physique et Analytique, Station 6, Ecole Polytechnique Fédérale de Lausanne, CH-1015, Lausanne, Switzerland

Corresponding author. E-mail: hubert.girault@epfl.ch

Impact of spotting on separation resolution and efficiency. To better assess the impact of the spotting process on the resolution, Table S-1 has been constructed. It relates the efficiency of several peaks as a function of the number of collected fractions. 5 peaks, covering the full separation window, have been chosen to study the impact of the spotting process on the separation efficiency. The chosen peaks are marked on the trace D of the Figure 2 in the main part of this manuscript.

	Fraction collection interval (s)			
	0	60	30	15
◇	566493	532340	519851	550647
□	61605	88577	77586	91000
X	165572	160540	144940	165237
○	108716	122963	107381	113958

Table S-1. Impact of the spotting process on the separation efficiency (number of theoretical plates/meter).

Same experimental conditions as in Figure 2 of the main part of the manuscript

Direct MALDI-TOF-MS of the test peptide mixture.

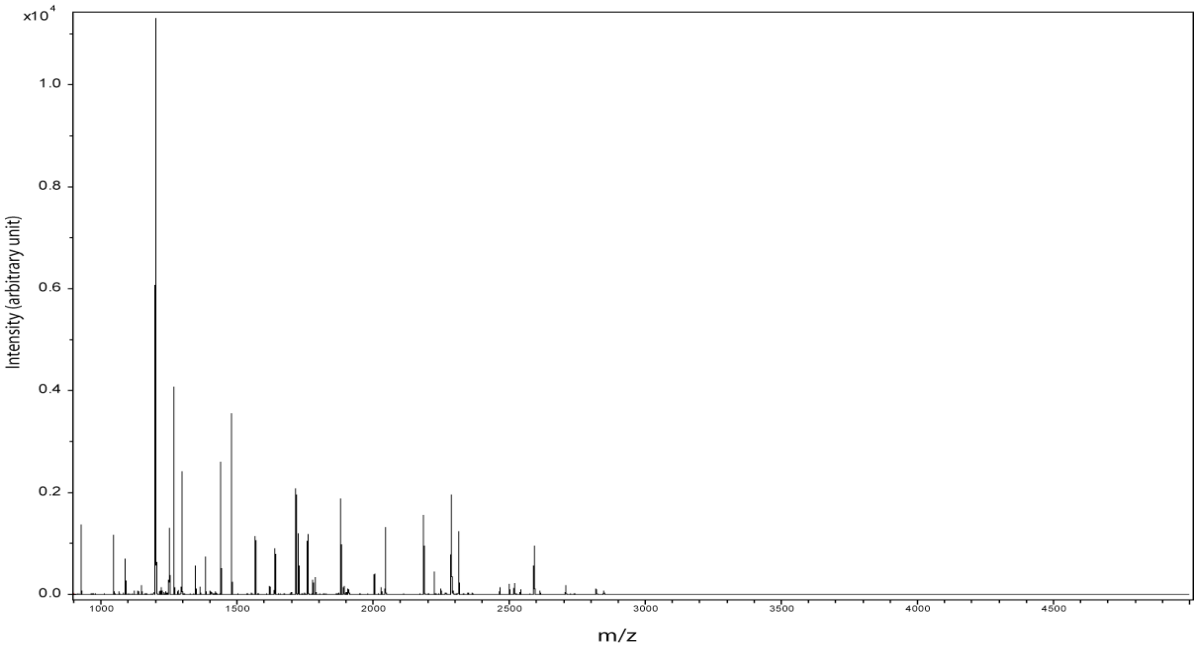

Figure S-1. MALDI-TOF mass spectrum of the total peptide mixture.

Sample: 0.5 µL of the Tryptic digest of total caseins (3.5 µM), α–□□□□□□□□□□□□(1.75 µM), β–□□□□□□□□□□□□□ (2.3 µM), bovine serum albumin (0.75 µM), ribonuclease A (3.75 µM). Sample and matrix application method as described in the materials and methods section.

List of the identified peptides. For the different experiments related in the main part of this article, the following tables mention the experimental and theoretical masses of the detected peptides, the mass accuracy, the corresponding sequences and each peptide position within the considered protein. The number of missed cleavage as well as existing modifications is specified. Finally, for each table corresponding to a CE-MALDI-MS experiment, the fraction in which each peptide has been detected is indicated.

CE-MALDI-TOF with direct spotting on MALDI target

Protein	CE fraction	Experimental mass (Da)	Theoritical mass (Da)	Mass accuracy (ppm)	Position	Sequence	Number of missed cleavage	Modifications
	11	1337.685	1337.6808	3.1	95-105	HIQKEDVPSER	1	
	13	910.461	910.4741	14.4	140-147	EGIHAQQK	0	
	27	1759.935	1759.9449	5.6	23-37	HQGLPQEVLNENLLR	0	
	28	1759.909	1759.9449	20.4	23-37	HQGLPQEVLNENLLR	0	
	31	1071.904	1071.9061	1.1	119-134	YKVPQLEIVPNSAEER	1	
αS1-casein	40	1267.681	1267.7045	18.5	106-115	YLGYLEQLLR	0	
	41	1267.676	1267.7045	22.5	106-115	YLGYLEQLLR	0	
	42	1267.701	1267.7045	2.8	106-115	YLGYLEQLLR	0	
	45	1384.73	1384.7299	0.1	38-49	FFVAPFPEVFGK	0	
	46	1384.763	1384.7299	23.9	38-49	FFVAPFPEVFGK	0	
	47	1384.711	1384.7299	13.6	38-49	FFVAPFPEVFGK	0	
	16	1246.633	1246.6426	7.7	86-95	TVDDKHYQK	1	
	17	1246.637	1246.6426	4.5	86-95	TVDDKHYQK	1	
	18	1246.652	1246.6426	7.5	86-95	TVDDKHYQK	1	
	31	979.546	979.5611	15.4	189-196	FALPQYLK	0	
αS2-casein	32	979.537	979.5611	24.6	189-196	FALPQYLK	0	
	33	979.541	979.5611	20.5	189-196	FALPQYLK	0	
	41	1195.666	1195.6793	11.1	130-140	NAVPITPTLNR	0	
	42	1367.676	1367.6954	14.2	96-106	ALNEINQFYQK	0	
	46	1351.73	1351.7804	37.3	129-140	RNAVPITPTLNR	1	
	59	1923.888	1923.9711	43.2	92-106	HYQKALNEINQFYQK	1	
β-casein	65	2186.071	2186.1678	44.3	199-217	DMPIQAFLLYQEPVLGPVR	0	
	17	1403.678	1403.626	37.0	32-42	CEKDERFFSDK	2	
k-casein	41	1251.682	1251.7096	22.0	46-55	YIPIQYVLSR	0	
	42	1251.708	1251.7096	1.3	46-55	YIPIQYVLSR	0	
	43	1251.725	1251.7096	12.3	46-55	YIPIQYVLSR	0	
	9	1200.62	1200.6524	27.0	118-127	VGINYWLAHK	0	
	16	1204.613	1204.603	8.3	134-142	LDQWLCEKL	1	Cys_CAM: 139
	17	1204.658	1204.603	45.7	134-142	LDQWLCEKL	1	Cys_CAM: 139
	18	1204.642	1204.603	32.4	134-142	LDQWLCEKL	1	Cys_CAM: 139
	19	1204.646	1204.603	35.7	134-142	LDQWLCEKL	1	Cys_CAM: 139
		1309.642	1309.6569	11.4	20-29	EQLTKCEVFR	1	Cys_CAM: 25
a-lactalbumin	20	1204.638	1204.603	29.1	134-142	LDQWLCEKL	1	Cys_CAM: 139
	24	2591.159	2591.1071	20.0	78-98	IWCKDDQNPHSSNICNISCD K	1	Cys_CAM: 80, 92, 96
	26	1827.815	1827.8503	19.3	99-113	FLDDDLTDDIMCVKK	1	Cys_CAM: 110
	27	1778.812	1778.8815	39.1	128-142	ALCSEKLDQWLCEKL	2	
	37	1252.595	1252.6354	32.3	20-29	EQLTKCEVFR	1	
	39	2297.253	2297.1403	49.1	99-117	FLDDDLTDDIMCVKKILDK	2	Cys_CAM: 110
	41	2420.116	2420.0428	30.2	78-98	IWCKDDQNPHSSNICNISCD K	1	
	19	1193.671	1193.6776	5.5	108-117	VLVLDTDYKK	1	
	20	1193.672	1193.6776	4.7	108-117	VLVLDTDYKK	1	
	28	1635.738	1635.7748	22.5	141-154	TPEVDDEALEKFDK	1	
	32	916.44	916.4734	36.4	100-107	IDALNENK	0	
	33	916.454	916.4734	21.2	100-107	IDALNENK	0	
	37	1121.44	1121.4607	18.5	77-85	WENGECAQK	0	Cys_CAM: 82
	39	2313.267	2313.2587	3.6	57-76	VYVEELKPTPEGDLEILLQK	0	
	40	2313.269	2313.2587	4.5	57-76	VYVEELKPTPEGDLEILLQK	0	
β-lactogobulin	41	2313.19	2313.2587	29.7	57-76	VYVEELKPTPEGDLEILLQK	0	
	49	1715.793	1715.8057	7.4	165-178	LSFNPTQLEEQCHI	0	Cys_CAM: 176
	50	1658.722	1658.7843	37.6	165-178	LSFNPTQLEEQCHI	0	
		1715.828	1715.8057	13.0	165-178	LSFNPTQLEEQCHI	0	Cys_CAM: 176
	51	1715.782	1715.8057	13.8	165-178	LSFNPTQLEEQCHI	0	Cys_CAM: 176
	56	1715.728	1715.8057	45.3	165-178	LSFNPTQLEEQCHI	0	Cys_CAM: 176
	57	1715.742	1715.8057	37.1	165-178	LSFNPTQLEEQCHI	0	Cys_CAM: 176
	66	2818.202	2818.2427	14.4	118-140	YLLFCMENSAEPEQSLACQC LVR	0	Cys_CAM: 122, 135, 137
	7	989.539	989.5486	9.7	58-65	SRNLTKDR	2	
	22	1504.669	1504.6736	3.1	112-124	ETGSSKYPNCAYK	1	Cys_CAM: 121
	23	1504.657	1504.6736	11.0	112-124	ETGSSKYPNCAYK	1	Cys_CAM: 121
	25	2517.239	2517.2224	6.6	66-87	CKPVNTFVHESLADVQAVCS QK	0	Cys_CAM: 66, 84
	26	2517.253	2517.2224	12.2	66-87	CKPVNTFVHESLADVQAVCS QK	0	Cys_CAM: 66, 84
	28	915.407	915.4029	4.5	118-124	YPNCAYK	0	Cys_CAM: 121
RNA	36	2224.058	2224.0855	12.4	131-150	HIIVACEGNPYVPVHFDASV	0	Cys_CAM: 136
	37	2224.12	2224.0855	15.5	131-150	HIIVACEGNPYVPVHFDASV	0	Cys_CAM: 136
	38	2224.051	2224.0855	15.5	131-150	HIIVACEGNPYVPVHFDASV	0	Cys_CAM: 136
	39	2223.98	2224.0855	47.4	131-150	HIIVACEGNPYVPVHFDASV	0	Cys_CAM: 136
	47	1501.765	1501.7104	36.4	118-130	YPNCAYKTQANK	1	
	62	2285.833	2285.922	38.9	93-111	NGQTNCYQSYSTMSITDCR	0	Cys_CAM: 98, 110
	9	1249.62	1249.6211	0.9	35-44	FKDLGEEHFK	1	
	10	1249.639	1249.6211	14.3	35-44	FKDLGEEHFK	1	
	11	2612.237	2612.1649	27.6	264-285	VHKECCHGDLLECADDRADL AK	2	Cys_CAM: 268, 269, 276
	12	1439.809	1439.8117	1.9	360-371	RHPEYAVSVLLR	1	
		2113.923	2113.8848	18.1	264-280	VHKECCHGDLLECADDR	1	Cys_CAM: 268, 269, 276
	13	1439.807	1439.8117	3.3	360-371	RHPEYAVSVLLR	1	
		1532.778	1532.7811	2.0	298-309	LKECCDKPLLEK	1	Cys_CAM: 301, 302
	14	1439.812	1439.8117	0.2	360-371	RHPEYAVSVLLR	1	
		1532.784	1532.7811	1.9	298-309	LKECCDKPLLEK	1	Cys_CAM: 301, 302
		1673.782	1673.77	7.2	118-130	QEPERNECFLSHK	1	Cys_CAM: 125
	16	1166.48	1166.4928	11.0	460-468	CCTKPESER	0	Cys_CAM: 460, 461
		1254.625	1254.5783	37.2	337-346	DVCKNYQEAK	1	Cys_CAM: 339
		2541.223	2541.1674	21.9	118-138	QEPERNECFLSHKDDSPDLP K	2	Cys_CAM: 125
	17	1254.614	1254.5783	28.5	337-346	DVCKNYQEAK	1	Cys_CAM: 339
		1308.666	1308.727	46.6	558-568	HKPKATEEQLK	1	
		2541.158	2541.1674	3.7	118-138	QEPERNECFLSHKDDSPDLP K	2	Cys_CAM: 125
	18	1193.63	1193.6021	23.4	25-34	DTHKSEIAHR	1	
		1254.621	1254.5783	34.0	337-346	DVCKNYQEAK	1	Cys_CAM: 339
		1901.851	1901.8698	9.9	123-138	NECFLSHKDDSPDLPK	1	Cys_CAM: 125
		2045.042	2045.0279	6.9	168-183	RHPYFYAPELLYYANK	1	
		2541.178	2541.1674	4.2	118-138	QEPERNECFLSHKDDSPDLP K	2	Cys_CAM: 125
	19	1283.71	1283.7106	0.5	361-371	HPEYAVSVLLR	0	
		1901.883	1901.8698	6.9	123-138	NECFLSHKDDSPDLPK	1	Cys_CAM: 125
		2020.012	2019.9691	21.2	139-155	LKPDPNTLCDEFKADEK	1	Cys_CAM: 147
		2045.014	2045.0279	6.8	168-183	RHPYFYAPELLYYANK	1	
	20	1283.713	1283.7106	1.9	361-371	HPEYAVSVLLR	0	
		1305.707	1305.7161	7.0	402-412	HLVDEPQNLIK	0	
		1795.817	1795.8319	8.3	387-401	DDPHACYSTVFDKLK	1	Cys_CAM: 392
		2019.962	2019.9691	3.5	139-155	LKPDPNTLCDEFKADEK	1	Cys_CAM: 147
	21	1305.718	1305.7161	1.5	402-412	HLVDEPQNLIK	0	
		1419.692	1419.6936	1.1	89-100	SLHTLFGDELCK	0	Cys_CAM: 99
	22	1419.69	1419.6936	2.5	89-100	SLHTLFGDELCK	0	Cys_CAM: 99
	23	1399.68	1399.6926	9.0	569-580	TVMENFVAFVDK	0	
		1419.676	1419.6936	12.4	89-100	SLHTLFGDELCK	0	Cys_CAM: 99
		1463.577	1463.5889	8.1	76-88	TCVADESHAGCEK	0	Cys_CAM: 77, 86
		2247.995	2247.9427	23.3	267-285	ECCHGDLLECADDRADLAK	1	Cys_CAM: 268, 269, 276
	24	1482.778	1482.7984	13.8	483-495	LCVLHEKTPVSEK	1	
	26	1576.737	1576.7675	19.3	139-151	LKPDPNTLCDEFK	0	Cys_CAM: 147
		1795.82	1795.8319	6.6	387-401	DDPHACYSTVFDKLK	1	Cys_CAM: 392
	29	1639.928	1639.9377	5.9	437-451	KVPQVSTPTLVEVSR	1	
BSA		1749.654	1749.6625	4.9	267-280	ECCHGDLLECADDR	0	Cys_CAM: 268, 269, 276
	30	1639.9	1639.9377	23.0	437-451	KVPQVSTPTLVEVSR	1	
		1880.935	1880.9211	7.4	508-523	RPCFSALTPDETYVPK	0	Cys_CAM: 510
	31	927.490	927.4934	2.0	161-167	YLYEIAR	0	
		1001.549	1001.589	39.9	233-241	ALKAWSVAR	0	
		1554.622	1554.6529	19.9	387-399	DDPHACYSTVFDK	0	Cys_CAM: 392
		1880.907	1880.9211	7.5	508-523	RPCFSALTPDETYVPK	0	Cys_CAM: 510
	32	927.475	927.4934	19.8	161-167	YLYEIAR	0	
		1880.878	1880.9211	22.9	508-523	RPCFSALTPDETYVPK	0	Cys_CAM: 510
		1907.874	1907.9207	24.5	529-544	LFTFHADICTLPDTEK	0	Cys_CAM: 537
	33	922.478	922.488	10.8	249-256	AEFVEVTK	0	
		927.493	927.4934	0.4	161-167	YLYEIAR	0	
		1068.446	1068.4415	4.2	413-420	QNCDQFEK	0	Cys_CAM: 415
		1907.868	1907.9207	27.6	529-544	LFTFHADICTLPDTEK	0	Cys_CAM: 537
	34	1107.515	1107.5139	1.0	588-597	EACFAVEGPK	0	Cys_CAM: 590
	35	1107.514	1107.5139	0.1	588-597	EACFAVEGPK	0	Cys_CAM: 590
	36	1138.537	1138.5673	26.6	223-232	CASIQKFGER	1	Cys_CAM: 223
		2003.782	2003.7779	2.0	106-122	ETYGDMADCCEKQEPER	1	Cys_CAM: 114, 115
	37	2003.786	2003.7779	3.6	106-122	ETYGDMADCCEKQEPER	1	Cys_CAM: 114, 115
	38	1163.604	1163.6306	22.9	66-75	LVNELTEFAK	0	
		2487.112	2487.1101	0.8	184-204	YNGVFQECCQAEDKGACLLP K	1	Cys_CAM: 191, 192, 200
	39	1163.633	1163.6306	2.1	66-75	LVNELTEFAK	0	
		2487.146	2487.1101	14.4	184-204	YNGVFQECCQAEDKGACLLP K	1	Cys_CAM: 191, 192, 200
		2492.302	2492.2642	15.2	45-65	GLVLIAFSQYLQQCPFDEHV K	0	Cys_CAM: 58
	40	1291.631	1291.602	22.5	300-309	ECCDKPLLEK	0	Cys_CAM: 301, 302
	41	2457.147	2457.1833	14.8	341-360	NYQEAKDAFLGSFLYEYSRR	2	
	46	1465.746	1465.6886	39.2	456-468	VGTRCCTKPESER	1	Cys_CAM: 460, 461
		2458.268	2458.1806	35.6	319-340	DAIPENLPPLTADFAEDKDV CK	1	Cys_CAM: 339
	47	1464.789	1464.774	10.2	221-232	LRCASIQKFGER	2	Cys_CAM: 223
		1479.818	1479.7954	15.3	421-433	LGEYGFQNALIVR	0	
		2458.121	2458.1806	24.2	319-340	DAIPENLPPLTADFAEDKDV CK	1	Cys_CAM: 339
	48	1479.783	1479.7954	8.4	421-433	LGEYGFQNALIVR	0	
	49	1502.61	1502.6137	2.5	375-386	EYEATLEECCAK	0	Cys_CAM: 383, 384
	50	1700.746	1700.7869	24.0	372-386	LAKEYEATLEECCAK	1	Cys_CAM: 383, 384
	52	1724.773	1724.8346	35.7	469-482	MPCTEDYLSLILNR	0	Cys_CAM: 471
	55	1567.744	1567.7427	0.8	347-359	DAFLGSFLYEYSR	0	
		1627.834	1627.7996	21.1	286-299	YICDNQDTISSKLK	1	
	56	1567.746	1567.7427	2.1	347-359	DAFLGSFLYEYSR	0	
		1627.825	1627.7996	15.6	286-299	YICDNQDTISSKLK	1	
	57	1567.739	1567.7427	2.4	347-359	DAFLGSFLYEYSR	0	
	63	2316.052	2316.0457	2.7	184-204	YNGVFQECCQAEDKGACLLP K	184-204	

Table S-2: CE-MALDI-TOF-MS of the peptide mixture with direct spotting on a MALDI target

Experimental conditions for CE: HPC coated capillary, total/effective length 80/21.5 cm x 50 μm I.D. Voltage : 30 kV, current : 12 μA, UV absorbance at 200 nm. BGE: 10% acetic acid. Sample: Tryptic digest of total caseins (14 μM), α–□□□□□□□□□□□□(11 μM), β–□□□□□□□□□□□□□□□ (9 μM), bovine serum albumin (3 μM), ribonuclease A (15 μM). Sample injection: 30 mbar 200 s. Leading electrolyte (ammonium acetate pH 4, 250 mM ionic strength) injection prior to sample injection : 30 mbar 40 s. See materials and methods section for MS experimental conditions

Direct MALDI-TOF analysis

Protein	CE fraction	Experimental mass (Da)	Theoritical mass (Da)	Mass accuracy (ppm)	Position	Sequence	Number of missed cleavage	Modifications
αS1-casein		1267.709	1267.7045	3.5	106-115	YLGYLEQLLR	0	
		1384.718	1384.7299	8.6	38-49	FFVAPFPEVFGK	0	
		1759.918	1759.9449	15.3	23-37	HQGLPQEVLNENLLR	0	
β-casein		2186.142	2186.1678	11.8	199 217	DMPIQAFLLYQEPVLGPVR	0	
κ-casein		1251.706	1251.7096	2.9	46-55	YIPIQYVLSR	0	
α-lactalbumin		1091.508	1091.519	10.1	134-141	LDQWLCEK	0	Cys_CAM: 139
		1200.64	1200.6524	10.3	118-127	VGINYWLAHK	0	
		1779.792	1779.8404	27.2	128-141	ALCSEKLDQWLCEK	1	Cys_CAM: 130, 139
		1892.864	1892.9244	31.9	128-142	ALCSEKLDQWLCEKL	2	Cys_CAM: 130, 139
		2591.163	2591.1071	21.6	78-98	IWCKDDQNPHSSNICNISCD K	1	Cys_CAM: 80, 92, 96
		2847.396	2847.432	12.6	118-141	VGINYWLAHKALCSEKLDQW LCEK	2	Cys_CAM: 130, 139
β-lactoglobulin		1121.479	1121.468	9.8	77-85	WENGECAQK	0	Cys_CAM: 82
		1635.745	1635.7748	18.2	141-154	TPEVDDEALEKFDK	1	
		1715.769	1715.8057	21.4	165-178	LSFNPTQLEEQCHI	0	Cys_CAM: 176
		2313.233	2313.2587	11.1	57-76	VYVEELKPTPEGDLEILLQK	0	
		2707.449	2707.3759	27.0	31-56	VAGTWYSLAMAASDISLLDA QSAPLR	0	
		2818.348	2818.2667	28.8	118-140	YLLFCMENSAEPEQSLACQC LVR	0	Cys_CAM: 122, 135, 137
RNA		1150.62	1150.6215	1.3	27-36	KETAAAKFER	2	
		2224.051	2224.0855	15.5	131-150	HIIVACEGNPYVPVHFDASV	0	Cys_CAM: 136
		2285.933	2285.922	4.8	93-111	NGQTNCYQSYSTMSITDCR	0	Cys_CAM: 98, 110
		2517.226	2517.2224	1.4	66-87	CKPVNTFVHESLADVQAVCS QK	0	Cys_CAM: 66, 84
BSA		927.499	927.4934	6.0	161-167	YLYEIAR	0	
		1249.607	1249.6211	11.3	35-44	FKDLGEEHFK	1	
		1283.701	1283.7106	7.5	361-371	HPEYAVSVLLR	0	
		1399.662	1399.6926	21.9	569-580	TVMENFVAFVDK	0	
		1419.674	1419.6936	13.8	89-100	SLHTLFGDELCK	0	Cys_CAM: 99
		1439.802	1439.8117	6.7	360-371	RHPEYAVSVLLR	1	
		1479.793	1479.7954	1.6	421-433	LGEYGFQNALIVR	0	
		1567.739	1567.7427	2.4	347-359	DAFLGSFLYEYSR	0	
		1639.908	1639.9377	18.1	437-451	KVPQVSTPTLVEVSR	1	
		1724.802	1724.8346	18.9	469-482	MPCTEDYLSLILNR	0	Cys_CAM: 471
		1880.896	1880.9211	13.3	508-523	RPCFSALTPDETYVPK	0	Cys_CAM: 510
		1907.871	1907.9207	26.0	529-544	LFTFHADICTLPDTEK	0	Cys_CAM: 537
		2003.767	2003.7779	5.4	106-122	ETYGDMADCCEKQEPER	1	Cys_CAM: 114, 115
		2045	2045.0279	13.6	168-183	RHPYFYAPELLYYANK	1	
		2247.911	2247.9427	14.1	267-285	ECCHGDLLECADDRADLAK	1	Cys_CAM: 268, 269, 276
		2541.201	2541.1674	13.2	118-138	QEPERNECFLSHKDDSPDLP K	2	Cys_CAM: 125

Table S-3: Direct-MALDI-TOF-MS of the peptide mixture

Sample: 0.5 μL of the Tryptic digest of total caseins (3.5 μM), α–□□□□□□□□□□□□(1.75 μM), β–□□□□□□□□□□□□□□□ (2.3 μM), bovine serum albumin (0.75 μM), ribonuclease A (3.75 μM). Spotting method as described in the materials and methods section.

Numerical model for diffusion-migration simulations. The diffusion-migration numerical simulations are decoupled in 2 steps, following a supporting electrolyte excess assumption. First, the electric potential distribution is calculated using the classical Laplace equation (1). Then, the calculated electric field is used in the transient Nernst-Plank equation (2) in order to determine the time evolution of the concentration distribution of the sample plug species.

$$\nabla \bullet (j) = \nabla \bullet (-\sigma \nabla \phi) = 0 \qquad (1)$$

$$\frac{\partial c_i}{\partial t} + \nabla \bullet \left(-D_{app} \nabla c_i - \frac{z_i F}{RT} D_i c_i \nabla \phi \right) = 0 \qquad (2)$$

where j is the electrical current density, ϕ the electrical potential, σ the solution conductivity, c_i the species concentration, D_i their diffusion coefficient, z_i their charge, F the Faraday constant, R the gas constant and T the temperature. In the droplet, an apparent diffusion coefficient D_{app} is introduced to take into account the microscopic chaotic motion, or "spontaneous" convection, following a concept introduced by Levich.[1] The effect of this microscopic fluid motion is non-negligible in macroscopically still solutions and acts as an apparent diffusion coefficient depending on the distance y from a solid wall:

$$D_{app} = D_i \left(1 + 1.507 \left(\frac{y}{\delta} \right)^4 \right) \qquad (3)$$

where δ is the thickness of the classical Nernst layer. Eq (3) illustrates that the diffusion coefficient is equal to its theoretical value in the stagnant layer ($y<\delta$) and vary in y^4 when y is larger than the diffusion layer thickness δ.

The solution is assumed to be isothermal without any macroscopic convection. To decouple the electric field calculation from the transport equation, a uniform conductivity is assumed due to the presence of the BGE.

This 2-D axi-symetrical model is implemented on the finite element software Flux-Expert® (Astek, Grenoble, France) and operated on a Linux PC. The geometry is a cross-section of the end of the capillary immersed in the drop (50 and 375 μm internal and external diameters, 1mm length with 500 μm immersed in the drop with 500 μm water below the end of the capillary). As standard values, a microscopic diffusion coefficient of 10^{-10} $m^2 \cdot s^{-1}$ is taken for the peptides with a net charge of 3. The diffusion layer thickness, previously determined to be 230 μm for $Fe(CN)_6^{4-}$, has been approximated to 150 μm for the present value of the peptide

diffusion coefficient ($\delta \propto D^{0.25}$).[1] The electrical field intensity in the capillary is 350 V/cm (370 V imposed between the top of the capillary and the electrode, assumed to be an equipotential). A mesh size from 5 µm in the capillary to 0.2 µm near the immersed edge and a time step of 0.5 ms are used for all the calculations.

Simulation of the iontophoretic spotting process. To improve the understanding of the reported iontophoretic spotting process, diffusion-migration simulations have been carried out. The spotting process has been simulated from the moment where a 1 mm sample plug arrives at the outlet of the capillary (Images A and F of the Figure S-2) and further performed to simulate a total collection time of 40 seconds. A peptide presenting average values of electrophoretic mobility and diffusion coefficient has been chosen for the calculation. (See the supplementary information for further details)

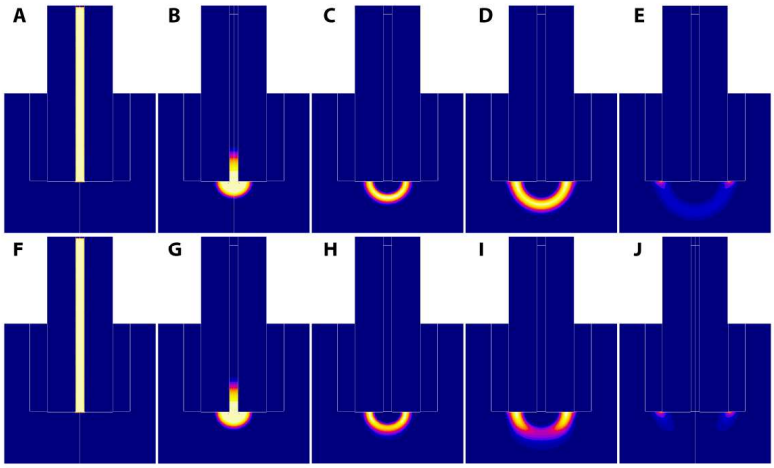

Figure S-2. Peptide concentration isovalues during the iontophoretic spotting process.

Figure S-2 represents the concentration isovalues of the chosen model peptide as a function of the spotting time in two different cases. The first case (Images A to E) deals with a situation where the spontaneous convection is considered negligible. In a second case (Images F to J), this effect is taken into account following Eq (3). Even if this increases the model accuracy, it has to be noticed that the macroscopic convection is undoubtedly playing a more important role in the present case. Indeed, in addition to the evaporation process, each

capillary manipulation (sequential dip and removal) certainly affects the droplet steadiness. Nevertheless, the iontophoretic spotting process can be well understood. As suggested by Figure S-2, the process can be divided into three steps. At first, the migrating peptide enters the collecting droplet by migrating in a crown-like zone. Then, depending on the magnitude of the convection, the crown-shape is more or less distorted in the vertical direction. Indeed, as can be seen on the images C,D and H,I, the further away the species are from the capillary, the higher the convection and the higher the dispersion. Finally, it can be observed that some of the collected species migrate toward the electrode (Images D,I, and E, J) where those species will be irreversibly attracted, the experimental drawback being certainly an increased carryover of the collected species from fraction to fraction. If the images E and J of Figure S-2 are compared, it can be suggested that the amount of peptides attracted by the electrodes is lower when the spontaneous convection is taken into account.

To further prove this last point, we have evaluated the amount of species, which can efficiently enter the collection droplet. To do so, we have calculated the flux of migrating and diffusing species across a virtual horizontal barrier. Experimentally, this barrier could be considered as the thickness of the film of liquid, which remains on the capillary when it is lift up from the droplet after a given collection time. As it was not experimentally possible to determine precisely this thickness, the calculations have been performed for different plausible values, ranging from 50 to 300 micrometers. An integration of the species flux as a function of the spotting time was carried out to estimate the percentage of species efficiently transferred to the collection droplet, the remaining corresponding to the proportion of species being potentially carried over till the next fraction. This simulation has been carried out for three collection periods, ranging from 10 to 40 seconds and the results are shown on Figure S-3.

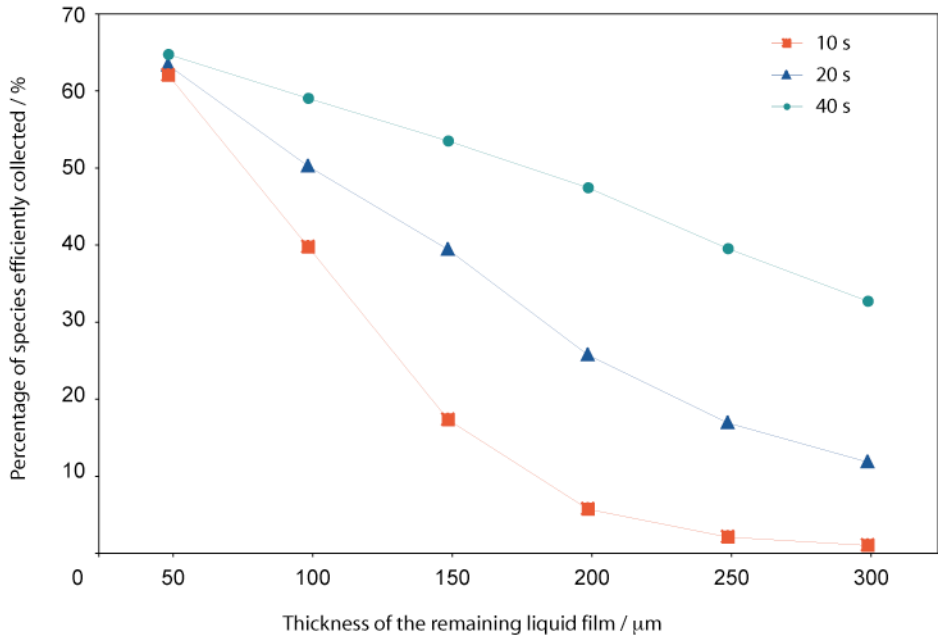

Figure S-3. Proportion of species efficiently collected as a function of the thickness of the remaining liquid film on the capillary outlet.

Figure S-3 demonstrates that the thickness of the film of liquid, which remains at the tip of the capillary, at the end of a collection period is certainly one of the most important parameter to be optimized when iontophoretic spotting is used. Indeed, for a short collection time of 10 s, the percentage of efficiently collected species can vary from about 60% to less than 10% when the film thickness is increased from 50 to 200 µm, as the species don't have time to cross the remaining film. This last case leads potentially to a significant carryover of the collected species from fraction to fraction. Then, if the collection time is gradually increased, it can be seen that the percentage of collected species increases. If this approach can constitute a solution for the analysis of a rather simple mixture, it is not the case for more complex ones, as the highest peak capacity will be required. Considering the results of this simulation part, it can be concluded that the coating of the outer outlet part of the separation capillary, has to be properly optimized as it can influence a lot the obtained results. Especially, in the case of electrophoretic separations carried out under high electric field or under conditions that induce large electrophoretic mobilites of the separated analytes, the outer coating of the

capillary outlet should insure the lowest film thickness while allowing current application when the capillary is moved from fraction to fraction.

1. Amatore, C.; Szunerits, S.; Thouin, L.; Warkocz, J. S. *J. of Electroanal. Chem.* **2001,** 500, 62-70